Chemical Engineering Journal 160 (2010) 164–169

Contents lists available at ScienceDirect

Chemical Engineering Journal

journal homepage: www.elsevier.com/locate/cej

Degradation of azo dyes using *in-situ* Fenton reaction incorporated into H_2O_2-producing microbial fuel cell

Lei Fu[a], Shi-Jie You[b], Guo-quan Zhang[a], Feng-Lin Yang[a,*], Xiao-hong Fang[a]

[a] Key Laboratory of Industrial Ecology and Environmental Engineering, MOE, School of Environmental and Biological Science and Technology, Dalian University of Technology, Dalian 116024, PR China
[b] State Key Laboratory of Urban Water Resources and Environments (SKLUWRE), Harbin Institute of Technology, Harbin 150090, PR China

ARTICLE INFO

Article history:
Received 21 December 2009
Received in revised form 8 March 2010
Accepted 16 March 2010

Keywords:
Microbial fuel cell
Fenton
Hydrogen peroxide
Amaranth
Iron reduction

ABSTRACT

This study investigated degradation of azo dyes by using microbial fuel cell (MFC)-Fenton system, in which *in-situ* production of H_2O_2 was achieved through two-electron reduction of oxygen in neutral catholyte. Based on sequential operation where H_2O_2 was synthesized followed by Fenton reaction, the MFC-conventional Fenton system was shown able to remove amaranth (75 mg/L) with the ratio of 82.59% within 1 h when 1 mmol/L Fe^{2+} was applied. For the MFC-electrochemical Fenton system with 0.5 mmol/L Fe^{3+} addition, the removal ratio of amaranth (75 mg/L) could reach 76.43% and cathode potential could keep stable for 1 h. Meanwhile, a maximum power density of 28.3 W/m^3 was obtained, which was larger than that of 17.2 W/m^3 when $K_3Fe(CN)_6$ was used as cathodic electron acceptor. This study suggests a proof-in-concept new manner for biorefractory wastewater treatment using the energy produced from biodegradable wastewater along with electrical energy generation simultaneously, which makes dye-containing wastewater treatment a green treatment process and more sustainable.

1. Introduction

The removal of toxic and biorefractory organic substances from groundwater and wastewater has been of great significance to prevent water environment from contamination of hazardous chemicals for years. Utilizing conventional methods to treat these substances, such as adsorption [1], coagulation [2], filtration [3] and sedimentation [4] have been proved to be technically feasible. However, these approaches may be problematic and unsustainable, due to potential production of various secondary wastes which need further treatments [5]. In recent years, advanced oxidation processes (AOP) have been widely developed as promising and efficient methods to treat aqueous recalcitrant organic pollutants [6–11]. Compared with other processes, AOP can offer several particular advantages such as high efficiency, easy operation and less production of residuals at the end of treatment. In general, AOP can be defined as a treatment process involving *in-situ* generation of hydroxyl radical (•OH) which has extremely great redox potential (E^0 = 2.80 V vs. NHE) to react non-selectively with organics to their final mineralization at near-ambient temperature and pressure [12]. The Fenton method has been widely applied as AOP process, which involves the use of aqueous mixtures of ferrous iron (Fe^{2+}) and hydrogen peroxide (H_2O_2) under acidic condition [Eq. (1)]. This method is more advantageous than other AOP processes because ironic element is highly abundant and non-toxic; as well, the degraded products of H_2O_2 is environmentally-benign [13,14].

$$Fe^{2+} + H_2O_2 \rightarrow Fe^{3+} + {}^{\bullet}OH + OH^- \qquad k = 63\ M^{-1}\ s^{-1} \tag{1}$$

However, several limitations may hamper the conventional Fenton (CF) system into commercial application. First, there can be economic obstacles due to the great cost of H_2O_2 and unsafe risks associated with the transport and handling of commercial concentrated H_2O_2. Second, massive iron sludge produced with the form of $Fe(OH)_3$ requires proper disposal, which needs additional investment for appropriate design and operation of the whole system. Recently, the indirect electro-oxidation method, i.e. electrochemical Fenton (EF) approach, is regarded as an effective alternative [15], by its virtue of the ability to supply *in-situ* H_2O_2 through two-electron oxygen reduction reaction (ORR) at the carbonaceous cathode [Eq. (2)].

$$O_2 + 2H^+ + 2e^- \rightarrow H_2O_2 \tag{2}$$

Additionally, in the process of EF, Fe^{2+} can also be continuously regenerated from the reduction of Fe^{3+} at the cathode as can be seen from Eq. (3) [16].

$$Fe^{3+} + e^- \rightarrow Fe^{2+} \tag{3}$$

* Corresponding author. Tel.: +86 411 84706328; fax: +86 411 84708083.
E-mail address: yangfl@dlut.edu.cn (F.-L. Yang).

1385-8947/$ – see front matter © 2010 Elsevier B.V. All rights reserved.
doi:10.1016/j.cej.2010.03.032

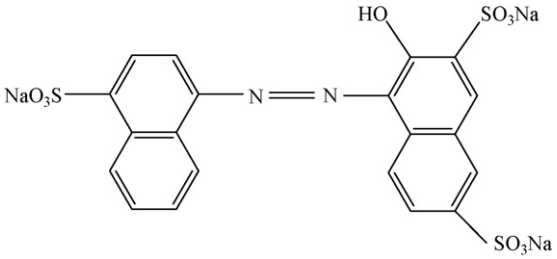

Fig. 1. Chemical structure of amaranth used in this study.

Although EF can overcome several disadvantages of CF, it is still an energy-intensive method, because of the requirement of high electrical voltage to achieve high removal efficiency.

Microbial fuel cell (MFC) is a completely new bioelectrochemical technology to treat wastewater [17], and the most remarkable advantage of MFC is its ability to generate combustion-less, pollution-free bioelectricity directly from biodegradable compounds by utilizing bacteria as catalysts [18]. Rozendal et al. [19] and our team [20] have found that, in addition to power yield, it was also possible to synthesize H_2O_2 in the catholyte of a MFC system with noble-metal-free graphite as cathode material. As a result, if H_2O_2 produced from MFC can be mixed with iron solution, a new external power-free EF system will be established, which gives rise to what we call MFC-Fenton system. Providing organic wastewater used as anodic fuel, using MFC-Fenton to degrade non-biodegradable chemicals such as dyes in biorefractory wastewater with energy produced from wastewater will be expected.

Dyes materials, which often constitute an important portion of wastewater effluent, are non-biodegradable and show a relatively high persistence in soils and aquatic systems. Azo dyes account for over 60% of the total number of dye structures known and salicylic acid derivatives of mordant azo dyes are numerically predominant [21]. As shown in Fig. 1, amaranth can be a typical representative of azo dyes, and its molecular structure determines the chemical stability and resistance to H_2O_2. Based on the above considerations, we chose amaranth as the target pollutant in this study.

The primary objective of this study is to construct a MFC-Fenton system for examining *in-situ* degradation of biorefractory organics (amaranth) along with power generation. First, we investigated effects of operational modes and amaranth on H_2O_2 production. Second, amaranth degradation was studied in the MFC-Fenton system by applying CF and EF method, with addition of Fe^{2+} and Fe^{3+} as Fenton catalysts, respectively.

2. Materials and methods

2.1. Chemicals and analyzes

Amaranth (A.G.) was purchased from Beijing Chemical Reagents Company and used without further purification. Other chemicals such as $FeSO_4{\cdot}7H_2O$, $Fe_2(SO_4)_3$, $TiOSO_4{\cdot}2H_2O$, $K_3Fe(CN)_6$, glucose, NH_4Cl, KCl, H_2SO_4, NaOH, NaH_2PO_4 and Na_2HPO_4 were analytic grade. High-purity gaseous O_2 and N_2 were used to maintain oxygen-saturated and deoxygenated conditions in the electrolyte. The aqueous pH was adjusted to desired levels by adding H_2SO_4 (0.5 M) or NaOH (1 M), and measured by pB-10 pH-meter (Sartorius AG, Germany).

H_2O_2 concentration was determined by spectrophotometry (722s, Jinghua, China) of titanium (IV) oxysulphonate–sulfuric acid complex ($TiOSO_4{\cdot}xH_2SO_4{\cdot}xH_2O$). Fe^{2+} concentration was measured by light absorbance at wavelength of 510 nm after complexion with 1,10-phenanthroline. Determination of amaranth concentration was performed spectrophotometrically by measuring the light absorbance at wavelength of 524 nm. TOC analyzes were carried out using a 5050 TOC-V_{CPH} analyzer (Shimadzu, Japan).

2.2. Electrochemical measurements

Cyclic voltammograms (CV) and electrochemical impedance spectroscopy (EIS) measurements were carried out using a Potentiostat/Galvanostat EG&G Model 263A and a frequency response detector FRD 100 of Princeton Applied Research. The working electrode was the cross section of spectrographic pure graphite (SPG) rod (Φ 10 mm) and the counter electrode was a platinum sheet (surface area 4 cm^2). A saturated calomel electrode (SCE) was supplied as the reference electrode. If not stated otherwise, all potentials were reported against SCE (245 mV vs. NHE) in this study. All the experiments were carried out at room temperature (20 °C).

2.3. MFC-Fenton system

A double-chambered MFC reactor was constructed with two uniform glass bottles having total volume of 80 mL for each. The anode chamber was filled with granular graphite (diameter of 6–8 mm, specific surface area of 4.12 cm^2/mL area to volume), while two SPG rods (6 cm in length and 1 cm in diameter) were fixed to serve as cathode in the cathode chamber. Thus, the wet volume of the anode and cathode compartment was 50 mL and 70 mL, respectively. The two compartments were separated by proton exchange membrane [Nafion 112 (Dupont, USA)] with sectional area of 9 cm^2. The MFC reactor was started up according to the procedures as described in our previously reported studies. The anode chamber was fed with glucose (700 mg/L COD) as fuel substrate.

H_2O_2-producing MFC was operated with external resistance of 20 Ω and O_2 was purged into the cathode chamber (electrolyte was 0.1 mol/L Na_2SO_4) to supply the oxygen needed for two-electron ORR. After 12 h operation, 73–80 mg/L H_2O_2 would be achieved, and this system had a stable operation performance [20]. In this study, catholyte was amaranth solution with 0.1 mol/L Na_2SO_4 as supporting electrolyte, and the other operational parameters were the same as the H_2O_2-producing MFC. In the experiment of CF, catholyte containing amaranth and H_2O_2 which generated *in-situ*, was extracted from the cathode chamber and then transferred into a beaker, adjusted to pH 3.0 and added Fe^{2+} to start the Fenton reaction. In the experiment of EF, the Fenton reaction with Fe^{3+} as catalyst reacted in the cathode chamber after H_2O_2 generation process, and replaced growth medium of the anode concurrently to maintain anode potential stable. Both CF and EF were stirred with a magnetic stirrer to enhance the mass transport.

Cell voltage and cathode potential of the MFC were measured with a multimeter (UT803, China) and a data acquisition system connected to a personal computer. Current is calculated using Ohm's law ($I = E_{cell}/R$). Polarization curve was obtained using voltammetry tests at the scan rate of 1 mV/s by a Potentiostat/Galvanostat EG&G Model 263A.

3. Results and discussion

3.1. The selection of operation modes

Electrochemical Fenton (EF) is an electro-oxidation method, in which H_2O_2 and Fe^{2+} can be on-site generated electrochemically, either separately or concurrently [22]. Generally, H_2O_2 generation and Fenton process operate simultaneously in EF [23–26], and thereby, H_2O_2 could be catalyzed to form •OH immediately. Since the optimal pH for Fenton reaction is generally in the range of 2.5–3.5 [27], H_2O_2 generation could be achieved at acidic solutions in EF. For example, Zhu and Ni [28] adopted this mode to degrade p-nitrophenol in a MFC, in which controlling pH of catholyte was

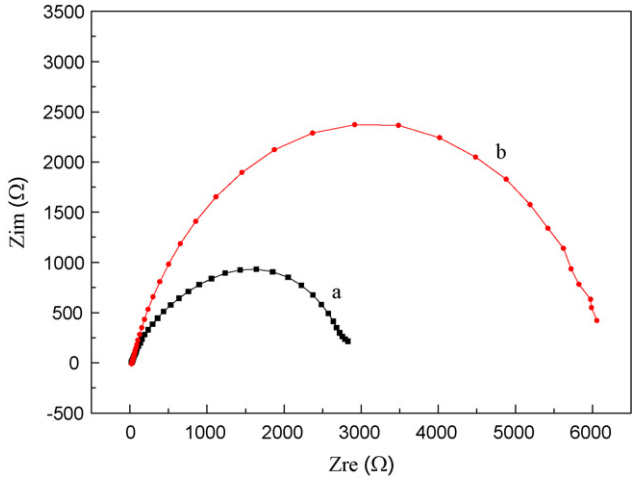

Fig. 2. EIS profile of SPG electrode in 0.1 mol/L Na_2SO_4 solution saturated with O_2 at the potential of −0.25 V at (a) pH 7.0 and (b) pH 3.0.

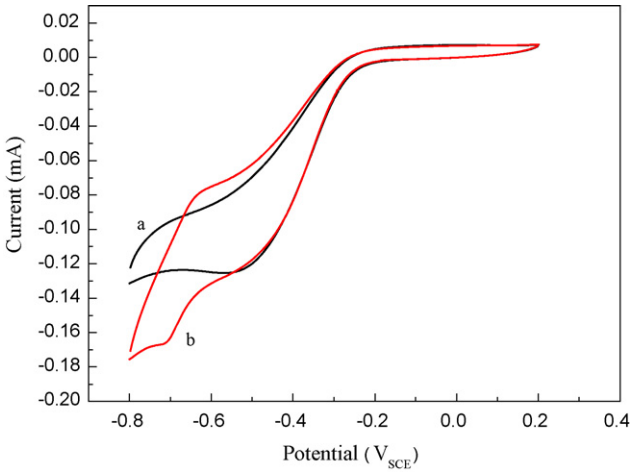

Fig. 3. Cyclic voltammogram (CV) scan of SPG electrode in 0.1 mol/L Na_2SO_4 solution saturated with O_2 at pH 7.0 in the (a) absence and (b) presence of 25 mg/L amaranth, Scan rate was 20 mV/s.

a significant factor for efficient H_2O_2 generation. Fig. 2 shows the EIS profile of SPG electrode in oxygen-saturated solutions at pH 7.0 and pH 3.0. The data were fitted and simulated by ZSimpWin3.10 software, which gave change transfer resistances (R_{ct}) for ORR of 2512 Ω (pH 7.0) and 5708 Ω (pH 3.0), respectively. Thus, the standard rate constant (K^0) of ORR at different pH can be derived from R_{ct} using Eq. (4) [29]:

$$K^0 = \frac{RT}{n^2F^2R_{ct}A\ C_{O_2}} \quad (4)$$

where R (8.314 J/mol K) is the ideal gas constant, T (293 K) the absolute temperature, n ($n = 2$) the mole number during two-electron reduction of oxygen, F (96485 C/mol) the Faraday's constant, A (0.785 cm^2) the area of the electrode, C_{O_2} (3×10^{-7} mol/cm^3) the bulk concentration of dissolved oxygen. As indicated in Eq. (4), K^0 is inversely proportional to R_{ct}, so $K^0{}_{pH\,7}$ was 2.27 times of $K^0{}_{pH\,3}$, suggesting that ORR reaction rate at SPG electrode in neutral electrolyte proceeds faster than that in acidic electrolyte. Operating H_2O_2-producing MFC using catholyte with different pH, the accumulated H_2O_2 concentration at initial pH 7 was observed 2.52 times of that obtained at initial pH 3, and this result appeared to be in a good agreement with EIS analysis. Taking into account of the importance of H_2O_2 amount for Fenton reaction and properties of H_2O_2 formation in the MFC using SPG as the electrode, operating the system under sequence mode was preferred to that under synchronization mode. In other words, to enable more efficient H_2O_2 yield, the system should be better off by synthesis of H_2O_2 in MFC in neutral catholyte, then followed by Fenton reaction through adjustment of catholyte pH to 3.0 and addition of ironic catalyst.

Fig. 3 illustrates the cyclic voltammograms (CV) scan of SPG electrode oxygen-saturated electrolyte (pH 7.0) in the absence and in the presence of amaranth (25 mg/L). It is clearly visible that the ORR currents of two cases were completely identical at the cathode potential higher than −0.4 V. As the operating cathode potential of H_2O_2-producing MFC was changed from −0.3 V to −0.2 V and cathode potentials appeared almost the same over the whole testing period without and with amaranth, it can be concluded that the presence of amaranth had slight impact on the ORR process occurring on the surface of the SPG rod. As a result, it can be concluded that the presence of amaranth had little impact on ORR process occurring on the surface of SPG rod. For H_2O_2-producing MFC being operated in the presence of amaranth in the catholyte without addition of Fe^{2+}, amaranth concentration did not show obvious change after a long time of period, which clearly suggested that H_2O_2 was unable to decompose amaranth without ironic catalyst.

3.2. MFC-conventional Fenton

3.2.1. Effect of Fe^{2+} concentration

According to Eq. (1), hydroxyl radical generation was mainly dependent upon both H_2O_2 and Fe^{2+} concentration. Considering that the amount of H_2O_2 generated from MFC could be assumed constant at defined conditions, Fenton reaction in this predefined system was dominated by Fe^{2+} concentration. The effect of Fe^{2+} concentration on amaranth degradation efficiency is given in Fig. 4(a). For initial amaranth concentration of 25 mg/L, Fe^{2+} was shown to have little influence on degradation efficiency (almost 100%) over a wide range from 0.5 to 3.0 mg Fe^{2+}/L. However, when Fe^{2+} concentration reached higher level of 5.0 mg/L, degra-

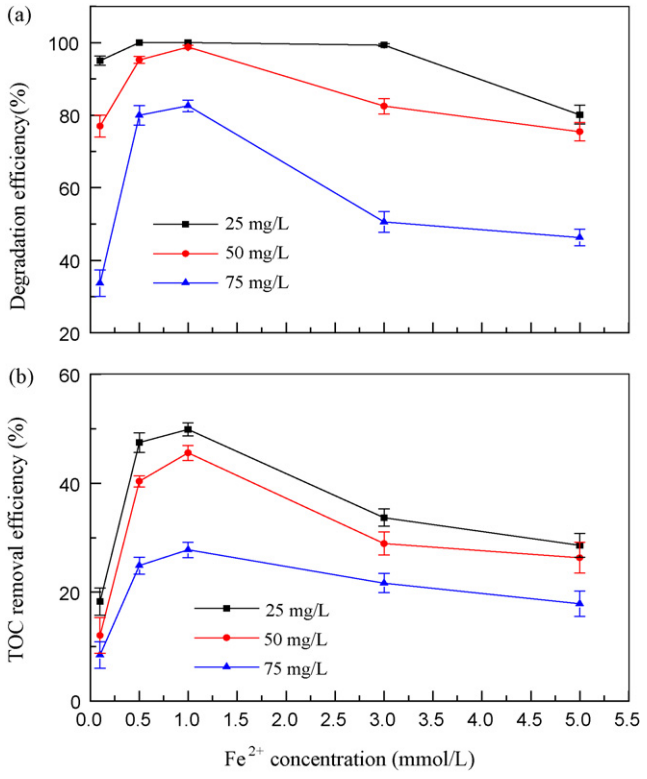

Fig. 4. Influences of Fe^{2+} concentration on (a) amaranth degradation and (b) TOC decay using Fe^{2+} as Fenton catalyst. pH 3.0 and reaction time = 1 h.

dation efficiency tended to decrease to 80.15%. The variation of degradation efficiency with Fe^{2+} addition demonstrated similar tendency for initial amaranth concentration of 50 mg/L and 75 mg/L. Degradation efficiency addressed a rapid increase when Fe^{2+} concentration increased from 0.1 mg/L to 1.0 mg/L and this should be attributed to an increase in the amount of hydroxyl radical generated with the increase of Fe^{2+} [Eq. (1)]. On the other hand, further increase of Fe^{2+} concentration in the range of 1.0–5.0 mg/L led to a gradual drop of degradation efficiency, due to the simultaneous consumption of hydroxyl radical by Fe^{2+} as shown in Eq. (5) [30]

$$Fe^{2+} + {}^{\bullet}OH \rightarrow Fe^{3+} + OH^{-} \qquad k = 3.2 \times 10^{8}\ M^{-1}\ s^{-1} \tag{5}$$

Although the rate constant of hydroxyl radical reaction with dyes as given in Eq. (6) is 1–2 order-of-magnitude greater than that of reaction with Fe^{2+}, excessive Fe^{2+} would also cause hydroxyl radical loss associated with Fe^{2+} oxidation, and thus decrease in efficiency of dyes decomposition [5].

$$RH + {}^{\bullet}OH \rightarrow R^{\bullet} + H_2O \qquad k = 10^{9}\text{–}10^{10}\ M^{-1}\ s^{-1} \tag{6}$$

Furthermore, excessive Fe^{2+} added generates massive hydroxyl radical instantaneously [Eq. (1)], and the hydroxyl radical produced could react with H_2O_2, [31]

$$^{\bullet}OH + H_2O_2 \rightarrow HO_2{}^{-} + HO_2{}^{\bullet} + H_2O \quad k = 2.7 \times 10^{7}\ M^{-1}\ s^{-1} \tag{7}$$

This side reaction also resulted in losses of H_2O_2 and hydroxyl radical simultaneously.

Fig. 4(b) presents the effects of Fe^{2+} on TOC removal efficiency, which are seen almost the same to that of amaranth degradation curves. The optimal performances in amaranth degradation and TOC removal could be obtained at 1.0 mg Fe^{2+}/L for the whole initial concentrations of amaranth. Much higher Fe^{2+} concentration might make TOC removal efficiency decline. In addition to the explanations mentioned above, the formation of Fe^{3+}–carboxylic acid complexes such as $Fe(C_2O_4)^{+}$, $Fe(C_2O_4)^{-}$ and $Fe(C_2O_4)_3{}^{3-}$ [32,33] that are difficult to be degraded by hydroxyl radical can also be another likely reason for decrease in TOC removal when Fe^{2+} concentration was increased. Hence, it should be of importance to control Fe^{2+} concentration at a suitable level to promote hydroxyl radical generation, and consequently improve efficiencies of amaranth degradation and mineralization. For the particular MFC system used here to treat amaranth, the optimal Fe^{2+} concentration was determined to be approximately 1.0 mg/L.

3.2.2. Effect of reaction time

Fig. 5 presents the time course of amaranth and TOC decay in the MFC-CF system. As is illustrated in Fig. 5(a), amaranth degradation efficiencies could reach 100%, 88.89% and 75.65% during initialized reaction time of 15 min for initial amaranth concentration of 25 mg/L, 50 mg/L and 75 mg/L, respectively. When reaction time prolonged to 120 min, degradation efficiencies were merely increased by 11.11% and 8.59% for initial amaranth concentration of 50 mg/L and 75 mg/L. The maximum amaranth degradation for initial concentration of 75 mg/L could be 84.24%, and this system should be more effective for the case of low amaranth concentration. As is showed in Fig. 5(b), TOC removal was achieved at faster rates within the initial 15 min than that within latter stage. Obviously visible is that the overall reaction of hydroxyl radical degrading azo dyes could be separated to two steps. The first step is the cleavage of azo bond to form aromatic ring molecules by hydroxyl radical, and then aromatic ring molecules are broken via oxidative ring opening reactions [34]. This reaction was known to proceed rapidly; as a result, majority of amaranth could be removed during the first time of 15 min. The second step is characterized by the degradation of short-chain carboxylic acids formed in the first step, which are difficultly oxidized by hydroxyl radical produced in Fenton reaction. Owing to the "platform behavior" effect [26], the maximum TOC removal efficiencies of only 56.09%, 48.09% and 31.08% were obtained for initial amaranth concentration of 25 mg/L, 50 mg/L and 75 mg/L, respectively.

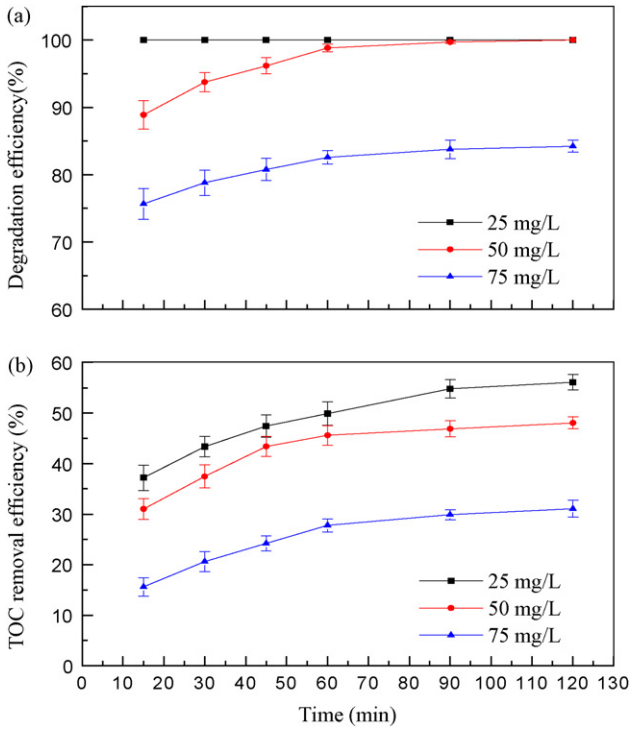

Fig. 5. Variation of (a) amaranth concentration and (b) TOC removal with reaction time using Fe^{2+} as Fenton catalyst. pH 3.0 and Fe^{2+} concentration = 1.0 mmol/L.

3.3. MFC-electrochemical Fenton

Another novel method being available to perform Fenton reaction in MFC is to incorporate electrochemical reduction of Fe^{3+} to Fe^{2+} to establish a Fenton system, where Fe^{3+} is used as the cathodic electron acceptor for MFC and its reduced intermediate Fe^{2+} plays a role of catalyst to participate Fenton reaction. Based on the optimal Fe^{2+} concentration of 1.0 mmol/L obtained above and regeneration of Fe^{3+} from Fe^{2+} oxidation at the cathode continuously, we fixed Fe^{3+} concentration as 0.5 mmol/L in the catholyte of MFC-EF system.

It can be seen from Fig. 6 that degradation curves for external resistance of 200 Ω, 500 Ω and 1000 Ω are almost coincident, and degradation rates for smaller external resistance appeared slightly higher. Degradation efficiencies could reach about 70% within the first phase of 1 h, and then increased slowly to about 85% within the latter 2 h. While for the MFC-EF reactor operated under open-circuit condition, Fe^{3+} failed to be reduced by cathodic electrode. In this case, Fenton reaction taking place in the cathode chamber should be Fenton-like reaction. Fig. 6 shows that amaranth degradation rate is linearly proportional to reaction time in Fenton-like process and considerably slower than that obtained with external resistances used.

Fig. 7(a) shows cathode potential curves of MFC-EF to treat amaranth in the catholyte. Varying trends of potential curves for different external resistance are seen principally similar. Following relative stability within the first time of 1 h, the potential showed substantial decrease after 1 h, particularly for the curves corresponding 500 Ω and 200 Ω. After cathode potential dropped rapidly

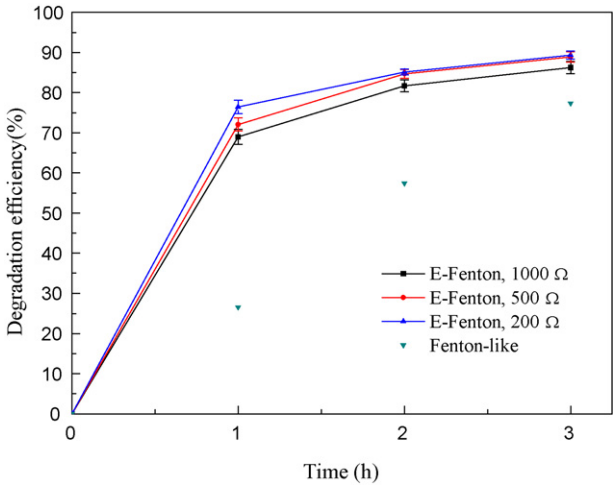

Fig. 6. Amaranth degradation efficiency as function of reaction time at external resistance of (a) 200 Ω, (b) 500 Ω, (c) 1000 Ω, and (d) open-circuit using Fe^{3+} as Fenton reaction catalyst. Experimental conditions: pH 3.0, amaranth concentration = 75 mg/L and Fe^{3+} concentration = 0.5 mmol/L.

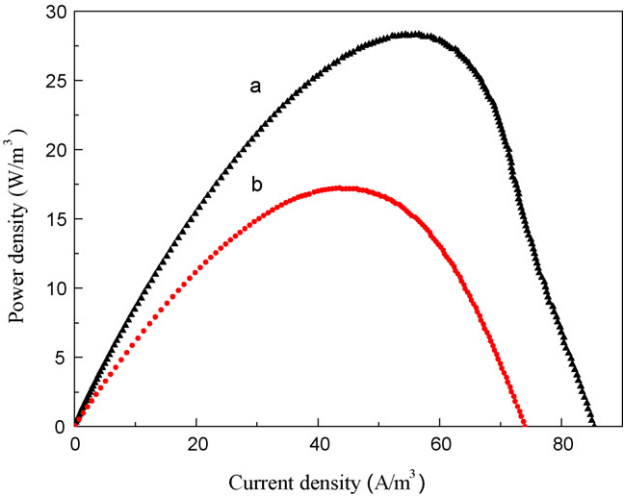

Fig. 8. Power density curves of (a) MFC-EF system at 0.5 mmol/L Fe^{3+}, pH 3.0, amaranth concentration = 75 mg/L and (b) MFC with 100 mmol/L $K_3Fe(CN)_6$, phosphate buffer.

to certain levels, curves were observed to shift gently at the end of tested phase.

The cathode potential time course of the MFC with cathode chamber only containing Fe^{3+} solution is given in Fig. 7(b), the difference with Fig. 7(a) is that cathode potential decreased at initial stage. Thereafter, to quantitatively analyze kinetics of Fe^{3+} reduction by cathodic electrode of MFC [Eq. (3)], Fe^{3+} concentration in the catholyte was measured at defined time intervals (data not shown). By performing kinetic analysis, the kinetic constants accounting for Fe^{3+} reduction in MFC were calculated to be 0.39 $M^{-1}\,s^{-1}$, 0.74 $M^{-1}\,s^{-1}$ and 1.20 $M^{-1}\,s^{-1}$ for external resistance of 1000 Ω, 500 Ω and 200 Ω, respectively.

It has been known that Fe^{3+} is incapable of catalyzing H_2O_2 directly to generate hydroxyl radical in Fenton-like reaction. Alternatively, hydroxyl radical is produced from H_2O_2 catalyzed by Fe^{2+} being reduced from Fe^{3+} [Eq. (8)]. [35]

$$Fe^{3+} + H_2O_2 \rightarrow Fe^{2+} + H^+ + HO_2^{\bullet} \qquad k = 2 \times 10^{-2}\,M^{-1}\,s^{-1} \qquad (8)$$

Kinetic constant of Fe^{3+} reduction by H_2O_2 is far less than that of Eq. (1) and Eq. (6), so Eq. (8) should be the rate-determining step of

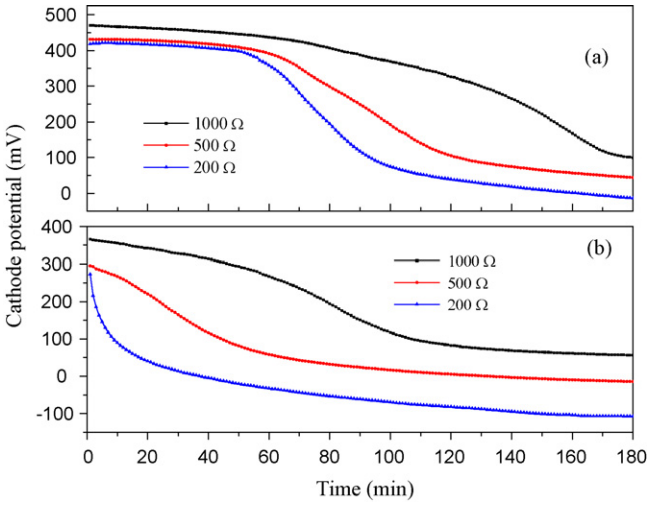

Fig. 7. Time profiles of cathode potential of (a) MFC-EF and (b) MFC system at various external resistances. Experimental conditions: pH 3.0, amaranth concentration = 75 mg/L and Fe^{3+} concentration = 0.5 mmol/L.

overall Fenton-like reaction. In MFC-EF system, Fe^{3+} can be reduced by cathodic electrode, and thus is still the rate-determining step compared with subsequent reactions. Nevertheless, Fe^{3+} reduction by cathodic electrode proceeds at a rate ($k = 10^{-1}$–$10^{0}\,M^{-1}\,s^{-1}$) much faster than that by H_2O_2. Therefore, this feature results in degradation rate of amaranth in MFC-EF being faster than that of Fenton-like reaction in MFC (Fig. 6). Following Fe^{2+} generation by cathodic electrode, it reacted immediately with H_2O_2 and generated hydroxyl radical. As a consequence, Fe^{2+} is converted to Fe^{3+} again [Eq. (1)]. Provided that H_2O_2 exists in the cathode chamber, concentration of Fe^{3+} could keep stable. This may provide an explanation to the question why cathode potential changed slightly at the initial phase in MFC-EF system [Fig. 7(a)]. Once the H_2O_2 was fully consumed, concentration of Fe^{3+} would start to decline, and so do the cathode potential. For the MFC whose cathode chamber only contained Fe^{3+} solution, Fe^{3+} could not be regenerated, so it is not surprising that the corresponding cathode potential dropped at the beginning of the scan [Fig. 7(b)]. After majority of Fe^{3+} has been reduced, further reduction seems likely more difficult because of great resistance from mass transfer. Qiang et al. examined regeneration of Fe^{2+} from Fenton reaction by using an electrolytic cell and they found that 75% of Fe^{2+} could be effectively regenerated with 25% remained Fe^{3+} that is hardly reduced [22]. This is seen well consistent with the results in Fig. 7 showing cathode potential curves presented declined tendency at end of record time. Hydroxyl radical generation in Fenton-EF is mainly in the first 1 h so that most of amaranth could be degraded within a short period of 1 h.

Stable power density curves of MFC-EF obtained within the first 1 h [Fig. 8(a)], demonstrated a maximum power density of 28.3 W/m^3 and defined internal resistance of 200 Ω. While for the same reactor with 100 mmol/L hexacyanoferrate as cathodic electron acceptor, the maximum power density was only 17.2 W/m^3, a value 39.2% lower than that produced from MFC-EF. Such difference should be likely a result of discrimination in standard potential of redox couple Fe^{3+}/Fe^{2+} ($E^0 = 0.77$ V vs. NHE) and $[Fe(CN)_6]^{3-}/[Fe(CN)_6]^{4-}$ ($E^0 = 0.36$ V vs. NHE).

Overall, development of MFC-EF system is in good consistence with the current tendency of sustainability and the ultimate goal of "design for environment" (DFE). By using this method, biodegradable wastewater and biorefractory can be possibly treated in one integrated system, together with output power concurrently. Another attractive feature of this system is that Fe^{3+} used as catalyst could be reused through dissolving iron sludge produced with

acidic solution. Therefore, there is no possibility and risk of secondary pollutant production from this system. The modified AOP explored on the basis of MFC concept for azo dyes degradation shown in this study offers a conceptually promising manner to treat biodegradable wastewater and biorefractory more economically and more sustainably.

4. Conclusions

Based on experimental results obtained in this study, some main conclusions could be made as follows.

(1) H_2O_2-producing MFC with neutral catholyte was able to generate more H_2O_2, so confirmed MFC-Fenton system operated with the mode of sequence, that is H_2O_2 generation first and then Fenton reaction.
(2) In MFC-conventional Fenton system, a majority of amaranth could be decomposed within 1 h, and the optimal concentration of Fe^{2+} was confirmed to 1.0 mmol/L.
(3) In MFC-electrochemical Fenton system, 0.5 mmol/L Fe^{3+} as catalyst, degradation efficiency of 75 mg/L amaranth could reach 76.4% within 1 h. The cathode potential of MFC-EF could keep stable and the maximum power density was up to 28.3 W/m^3, which is larger than that of MFC with $K_3Fe(CN)_6$ as electron acceptor.

Acknowledgements

We would give our gratitude to Shu-zhen Du and Ting-ting Liao for their valuable helps to this study.

References

[1] Y.S. Ho, T.H. Chiang, Y.M. Hsueh, Removal of basic dye from aqueous solution using tree fern as a biosorbent, Process Biochem. 40 (2005) 119–124.
[2] A. Alinsafi, M. Khemis, M.N. Pons, J.P. Leclerc, A. Yaacoubi, A. Benhammou, A. Nejmeddine, Electro-coagulation of reactive textile dyes and textile wastewater, Chem. Eng. Process. 44 (2005) 461–470.
[3] J.H. Mo, Y.H. Lee, J. Kim, J.Y. Jeong, J. Jegal, Treatment of dye aqueous solutions using nanofiltration polyamide composite membranes for the dye wastewater reuse, Dyes Pigments 76 (2008) 429–434.
[4] A.N.M. Bagyo, H. Arai, T. Miyata, Radiation-induced decoloration and sedimentation of colloidal disperse dyes in water, Appl. Radiat. Isot. 48 (1997) 175–181.
[5] M.A. Rauf, S.S. Ashraf, Radiation-induced degradation of dyes–An overview, J. Hazard. Mater. 166 (2009) 6–16.
[6] F.H. Abdullah, M.A. Rauf, S. Salman Ashraf, Photolytic oxidation of Safranin-O with H_2O_2, Dyes Pigments 72 (2007) 349–352.
[7] V. Flotron, C. Delteil, Y. Padellec, V. Camel, Removal of sorbed polycyclic aromatic hydrocarbons from soil, sludge and sediment samples using the Fenton's reagent process, Chemosphere 59 (2005) 1427–1437.
[8] F.J Benitez, F.J. Real, J.L. Acero, A.I. Leal, C. Garcia, Gallic acid degradation in aqueous solutions by UV/H_2O_2 treatment, Fenton's reagent and the photo-Fenton system, J. Hazard. Mater. 126 (2005) 31–39.
[9] J. Wu, T. Wang, Ozonation of aqueous azo dye in a semi-batch reactor, Water Res. 35 (2001) 1093–1099.
[10] M. Goel, H. Hongqiang, A.S. Mujumdar, M.B. Ray, Sonochemical decomposition of volatile and non-volatile organic compounds—a comparative study, Water Res. 38 (2004) 4247–4261.
[11] M. Saquib, M. Abu Tariq, M. Faisal, M. Muneer, Photocatalytic degradation of two selected dye derivatives in aqueous suspensions of titanium dioxide, Desalination 219 (2008) 301–311.
[12] W.H. Glaze, J.W. Kang, D.H. Chapin, The chemistry of water treatment processes involving ozone, hydrogen peroxide and ultraviolet radiation, Ozone: Sci. Eng. 9 (1987) 335–352.
[13] C.K. Duesterberg, T.D. Waite, Process optimization of Fenton oxidation using kinetic modeling, Environ. Sci. Technol. 40 (2006) 4189–4195.
[14] H. Gallard, J. De Laat, B. Legube, Effect of pH on the oxidation rate of organic compounds by FeII/H_2O, New J. Chem. (1998) 263–268.
[15] M.A. Oturan, J. Pinson, Hydroxylation by electrochemically generated OH. bul. radicals. Mono-and polyhydroxylation of benzoic acid: products and isomer distribution, J. Phys. Chem. 99 (1995) 13948–13954.
[16] I. Sires, N. Oturan, M.A. Oturan, R.M. Rodríguez, J.A. Garrido, E. Brillas, Electro-Fenton degradation of antimicrobials triclosan and triclocarban, Electrochim. Acta 52 (2007) 5493–5503.
[17] B.E. Logan, B. Hamelers, R. Rozendal, U. Schroder, J. Keller, S. Freguia, P. Aelterman, W. Verstraete, K. Rabaey, Microbial fuel cells: methodology and technology, Environ. Sci. Technol. 40 (2006) 5181–5192.
[18] B.E. Rittmann, Opportunities for renewable bioenergy using microorganisms, Biotechnol. Bioeng. 100 (2008) 203–212.
[19] R.A. Rozendal, E. Leone, J. Keller, K. Rabaey, Efficient hydrogen peroxide generation from organic matter in a bioelectrochemical system, Electrochem. Commun. 11 (2009) 1752–1755.
[20] L. Fu, S. You, F. Yang, Synthesis of hydrogen peroxide in microbial fuel cell, J. Chem. Technol. Biol. in press doi:10.1002/jctb2367.
[21] J. He, W. Ma, J. He, J. Zhao, J.C. Yu, Photooxidation of azo dye in aqueous dispersions of H_2O_2/[alpha]-FeOOH, Appl. Catal. B-Environ. 39 (2002) 211–220.
[22] Z. Qiang, J.H. Chang, C.P. Huang, Electrochemical regeneration of Fe^{2+} in Fenton oxidation processes, Water Res. 37 (2003) 1308–1319.
[23] M.A. Oturan, J. Pinson, M. Traikia, D. Deprez, The electrochemical oxidation of riluzole, a neuroprotective drug: comparison with the reaction with oxygen derived radicals, J. Chem. Soc., Perkin Trans. 2 (1999) 619–622.
[24] E. Brillas, R. Sauleda, J. Casado, Degradation of 4-chlorophenol by anodic oxidation, electro-Fenton, photoelectro-Fenton, and peroxi-coagulation processes, J. Electrochem. Soc. 145 (1998) 759–765.
[25] G. Zhang, F. Yang, M. Gao, X. Fang, L. Liu, Electro-Fenton degradation of azo dye using polypyrrole/anthraquinonedisulphonate composite film modified graphite cathode in acidic aqueous solutions, Electrochim. Acta 53 (2008) 5155–5161.
[26] G. Zhang, F. Yang, L. Liu, Comparative study of Fe_2+/H_2O_2 and Fe_3+/H_2O_2 electro-oxidation systems in the degradation of amaranth using anthraquinone/polypyrrole composite film modified graphite cathode, J. Electroanal. Chem. 632 (2009) 154–161.
[27] R. Andreozzi, V. Caprio, A. Insola, R. Marotta, Advanced oxidation processes (AOP) for water purification and recovery, Catal. Today 53 (1999) 51–59.
[28] X. Zhu, J. Ni, Simultaneous processes of electricity generation and *p*-nitrophenol degradation in a microbial fuel cell, Electrochem. Commun. 11 (2009) 274–277.
[29] M. Gao, F. Yang, G. Zhang, L. Liu, X. Wang, Effects of poly-1,5-diaminoanthraquinone morphology on oxygen reduction in acidic solution, Electrochim. Acta (2009) 2224–2228.
[30] Y. Sun, J.J. Pignatello, Photochemical reactions involved in the total mineralization of 2,4-D by iron(3+)/hydrogen peroxide/UV, Environ. Sci. Technol. 27 (1993) 304–310.
[31] G.V. Buxton, C.L. Greenstock, W.P. Helman, A.B. Ross, Critical review of rate constants for reactions of hydrated electrons, hydrogen atoms and hydroxyl radicals ($^{\bullet}OH/^{\bullet}O^-$) in aqueous solution, J, Phys. Chem. Ref. Data 17 (1988) 513–886.
[32] E. Brillas, J.C. Calpe, J. Casado, Mineralization of 2,4-D by advanced electrochemical oxidation processes, Water Res. 34 (2000) 2253–2262.
[33] I. Sires, F. Centellas, J.A. Garrido, R.M. Rodriguez, C. Arias, P.L. Cabot, E. Brillas, Mineralization of clofibric acid by electrochemical advanced oxidation processes using a boron-doped diamond anode and Fe2+ and UVA light as catalysts, Appl. Catal. B-Environ. 72 (2007) 373–381.
[34] E. Guivarch, S. Trevin, C. Lahitte, M.A. Oturan, Degradation of azo dyes in water by Electro-Fenton process, Environ. Chem. Lett. 1 (2003) 38–44.
[35] F. Chen, W. Ma, J. He, J. Zhao, Fenton degradation of malachite green catalyzed by aromatic additives, J. Phys. Chem. A 106 (2002) 9485–9490.